Curr Microbiol (2016) 73:904–914
DOI 10.1007/s00284-016-1138-1

Deletion of *pilA*, a Minor Pilin-Like Gene, from *Xanthomonas citri* subsp. *citri* Influences Bacterial Physiology and Pathogenesis

Silvana Petrocelli[1] · Maite R. Arana[1] · Marcela N. Cabrini[2] · Adriana C. Casabuono[2] · Laura Moyano[1] · Matías Beltramino[1] · Leandro M. Moreira[3,4] · Alicia S. Couto[2] · Elena G. Orellano[1]

Received: 14 April 2016 / Accepted: 13 September 2016 / Published online: 24 September 2016

Abstract Type IV pili (Tfp) are widely distributed adhesins of bacterial surfaces. In plant pathogenic bacteria, Tfp are involved in host colonization and pathogenesis. *Xanthomonas citri* subsp. *citri* (Xcc) is the phytopathogen responsible for citrus canker disease. In this work, three Tfp structural genes, *fimA*, *fimA1*, and *pilA* from Xcc were studied. A *pilA* mutant strain from Xcc (*XccΔpilA*) was constructed and differences in physiological features, such as motilities, adhesion, and biofilm formation, were observed. A structural study of the purified Tfp fractions from Xcc wild-type and *XccΔpilA* showed that pilins are glycosylated in both strains and that FimA and FimA1 are the main structural components of the pili. Furthermore, smaller lesion symptoms and reduced bacterial growth were produced by *XccΔpilA* in orange plants compared to the wild-type strain. These results indicate that the minor pilin-like gene, *pilA*, is involved in Tfp performance during the infection process.

Electronic supplementary material The online version of this article (doi:10.1007/s00284-016-1138-1) contains supplementary material, which is available to authorized users.

✉ Elena G. Orellano
orellano@ibr-conicet.gov.ar

[1] Facultad de Ciencias Bioquímicas y Farmacéuticas, Instituto de Biología Molecular y Celular de Rosario (IBR), Consejo Nacional de Investigaciones Científicas y Técnicas (CONICET), Universidad Nacional de Rosario, Suipacha 531, S2002LRK Rosario, Argentina

[2] Departamento de Química Orgánica, Facultad de Ciencias Exactas y Naturales, Centro de Investigaciones en Hidratos de Carbono, Universidad de Buenos Aires, 1428 Buenos Aires, Argentina

[3] Departamento de Ciências Biológicas (DECBI), Instituto de Ciências Exatas e Biológicas, Campus Morro do Cruzeiro, Universidade Federal de Ouro Preto, Ouro Preto, MG, Brazil

[4] Núcleo de Pesquisas em Ciências Biológicas (NUPEB), Universidade Federal de Ouro Preto, Ouro Preto, MG, Brazil

Introduction

Adhesion of pathogenic bacteria to eukaryotic cells is an essential step in the successful colonization of host tissue. The bacterial surface structures involved in adhesion include a broad group of fimbrial and non-fimbrial adhesins. Fimbrial adhesins, also known as pili, are hair-like appendages found on the surface of many bacteria. There are several types of pili, which differ in their mechanisms of assembly, structure, and function. Type IV pili (Tfp) are proteinaceous, flexible filaments with a diameter of 5–8 nm, which extend up to several micrometers in length and are generally located at one or both poles of a cell. These filaments are mainly composed of thousands copies of a small protein subunit named pilin, in most cases known as PilA [20]. Among fimbrial adhesins, Tfp are found in both gram-negative bacteria such as *Neisseria* spp., *Pseudomonas aeruginosa*, and enteropathogenic *Escherichia coli*, and in gram-positive bacteria such as *Clostridium* and *Streptococcus* species [20]. Tfp have been shown to be involved not only in bacterial adherence to eukaryotic cells but also in a variety of other bacterial functions such as natural transformation competence and a form of flagella-independent cell translocation known as twitching motility. In addition, twitching can be important for autoaggregation, biofilm formation, and multicellular development bodies. This motility is also required for host colonization and pathogenesis process, including the activation of host cell responses. These features make Tfp one

of the most studied pili and an interesting target for pathogens inhibition [5].

The study of Tfp and its role in pathogenesis was focused mainly on animal pathogenic bacteria. However, the role of Tfp in the virulence process of plant pathogenic bacteria is poorly understood. In fact, contributions of this structure to virulence have been reported mainly in vascular plant pathogens. A substantial role of Tfp in virulence was demonstrated for the pathogen *Ralstonia solanacearum* [25]. Besides, evidences of Tfp contribution to host colonization were reported for *Xylella fastidiosa* [32] and for *Pseudomonas syringae* pv. *tabaci* [51].

Xanthomonas citri subsp. *citri* (Xcc) is the phytopathogen responsible for citrus canker, one of the most devastating citrus diseases [4, 23]. The complete genomes of some plant pathogenic Xanthomonads have been sequenced [9, 30, 37, 52] and several genes involved in the virulence process were detected. Previous studies determined the role of many structures and proteins of *X. citri* subsp. *citri* in the virulence process [14, 16, 22, 53]. In addition, a plant natriuretic peptide [21], a characteristic lipopolysaccharide [7, 41], and the presence of a higher number of photoreceptors [27, 28] only present in Xcc genome were also evaluated.

Tfp contribution to virulence was studied in some *Xanthomonas* species. As a result, an important role of Tfp during the pathogenesis process was found in several cases, including *Xanthomonas campestris* pv. *campestris*, *Xanthomonas oryzae* pv. *oryzae*, *Xanthomonas oryzae* pv. *oryzicola*, and *X. citri* subsp. *citri* [10, 15, 35, 54].

In this study, three genes related to the structural subunit of Tfp in Xcc genome, *fimA*, *fimA1*, and *pilA* were identified. In order to determine the importance of PilA in bacterial physiology and its involvement in plant colonization during citrus canker, an Xcc mutant strain defective in *pilA* gene (*XccΔpilA*) was constructed. Also, an analysis of the glycosylation profile and peptide composition of pilin proteins from the wild-type and the mutant strains was performed.

Materials and Methods

Bacterial Strains, Culture Conditions, and Media

X. citri subsp. *citri* (Hasse) strain used in this work was derivative of the strain Xcc 99–1330, which was kindly provided by Blanca I. Canteros (INTA Bella Vista, Argentina).

Xcc strains were grown aerobically at 28 °C with shaking at 200 rpm in Silva Buddenhagen (SB) medium [11] or in the minimal medium XVM2 [55] supplemented with the corresponding antibiotics. *E. coli* cells were aerobically cultivated at 37 °C in Luria–Bertani medium. Antibiotics were used at the following final concentrations: ampicillin, 100 μg/ml for *E. coli* and 25 μg/ml for Xcc; kanamycin, 40 μg/ml; and streptomycin, 50 μg/ml. For *XccΔpilA(pBBad22K)*-complemented strain growth, SB medium was supplemented with 1 % (w/v) L-arabinose.

Recombinant DNA and Microbiological Techniques

All DNA manipulations including plasmid purification, restriction enzyme digestion, DNA ligation, and agarose gel electrophoresis were performed with standard techniques [44] unless otherwise specified. Total bacterial genomic DNA was isolated by the cetyltrimethylammonium bromide procedure [38]. Plasmids for bacterial conjugations were transferred to Xcc by biparental mating from the broad host range-mobilizing *E. coli* strain S17-1 [47]. Bacterial mixtures were spotted onto Hybond-C membranes, placed on SB agar and incubated for 48 h at 28 °C. Membranes were then washed and bacteria transferred to a selective medium as previously described [14].

Construction of the *XccΔpilA* Mutant Strain

The *XccΔpilA* mutant was constructed by insertional inactivation of the *pilA* gene (XAC3805, accession number AAM38647) on the chromosome due to the introduction of a streptomycin/spectinomycin resistance cassette as previously described by Kraiselburd et al. [27]. Primers used in this work are listed in Online Resource 1. Mutants were verified by PCR using the specific primers pilAF/R located on the coding region of the gene fragment. For mutant complementation, a 405-bp DNA fragment containing the *pilA*-coding region was amplified using the primer pair pilAF3/pilAR. The amplified DNA fragment was then cloned into the broad host range L-arabinose-inducible expression vector pBBad22K [50] to generate the recombinant plasmid pBBad/pilA. This plasmid was transferred into the *XccΔpilA* mutant strain by conjugation, producing *XccΔpilA(pBBad22K)* strain.

Quantification of Exopolysaccharide Production

Exopolysaccharide (EPS) production of Xcc strains was quantified as previously described by Petrocelli et al. [41].

Bacterial Motility Assays

Swimming and swarming assays were performed as previously described by Petrocelli et al. [41].

Twitching motility was analyzed as described by Kraiselburd et al. [46]. The zone of motility was visualized macroscopically and the morphology of colony edge was visualized microscopically by an optic Olympus BX40 microscope equipped with an Olympus camera system.

Bacterial Adhesion to Abiotic and Biotic Surfaces

For bacterial adherence to a plastic surface and to leaf surfaces, cultures of Xcc wild-type, *XccΔpilA* and *XccΔpilA(pBBad22K)* were grown overnight in liquid XVM2 medium and the cell attachment was evaluated as previously described by Petrocelli et al. [41].

Biofilm Formation Assay

In order to study biofilm formation, 20 µl of each saturated bacterial culture (10^9 colony-forming units (CFU)/ml) was transferred to glass tubes containing 2 ml of fresh medium, and then statically incubated at 28 °C. Bacterial aggregates were visually examined after 3 and 6 days of incubation. At each time, the tubes were incubated at 60 °C during 20 min. After the medium removal, bacteria were washed with sterile water and stained with a solution of 0.1 % (w/v) crystal violet (CV) for 45 min. Finally, the CV dye was solubilized by the addition of 95 % (v/v) ethanol and quantified by measuring absorbance at 540 nm [18].

Pili Extraction from Xcc wt and *XccΔpilA*

Bacterial strains were streaked on freshly poured XVM2 plates and incubated at 28 °C for 24 h. Bacteria were washed off in a small volume of distilled water, and the cell suspension was forced through a 25-gage hypodermic needle five times. Bacteria were removed by centrifugation (twice for 30 min, 23,300 *g*). The pili were collected by ultracentrifugation (twice for 60 min, 136,000 *g*), and the two pellets were separately suspended in 50 µl of 1 × SDS loading buffer (10 % (v/v) glycerol, 0.02 % (w/v) bromophenol blue, 25 µM DTT, 5 µM EDTA, and 2 % (w/v) SDS) [25].

Glycoprotein Digestion

Samples obtained from pili extraction were applied onto a 12 % SDS-PAGE. The protein bands were reduced with 10 mM DTT, further washed with acetonitrile and alkylated with 55 mM IAA in 50 mM NH_4HCO_3. The gel slices were digested in 20 ng/µl trypsin (Sigma) at 37 °C overnight [40]. Peptides were extracted by sonication with 50 % (v/v) acetonitrile in 1 % (v/v) trifluoroacetic acid (TFA), and the supernatant was taken to dryness.

In Gel-Reductive β-Elimination

The gel band was treated with 0.05 M NaOH/1 M $NaBH_4$ (0.5 ml) at 50 °C during 16 h. The solution was separated, acetic acid was added until pH 7 followed by repeated evaporation with methanol. The sample was dissolved in water, desalted in a Dowex 50 W (H^+) (Fluka) column, and dried in speed vac.

Acid Hydrolysis and Analysis of Monosaccharide Composition by HPAEC-PAD

A sample of the trypsin-released material was hydrolyzed with 2 N TFA for 2 h at 100 °C and sugars were analyzed by HPAEC-PAD in a DX-500 Dionex BioLC system (Dionex Corp.) with a pulse amperometric detector. The following conditions were employed: (a) for monosaccharides a carbopack P-20 column equipped with a P-20 precolumn eluted with a 16 mM NaOH isocratic program and a flow rate of 0.5 ml/min. (b) for oligosaccharides, a carbopack P-200 column equipped with a P-200 precolumn using a gradient elution with 100 mM NaOH, 0–29 % sodium acetate for 29 min and a flow rate of 0.4 ml/min.

Mass Spectrometry Analysis

Matrix and calibrating chemicals were purchased from Sigma-Aldrich. Measurements were performed using an Ultraflex II TOF/TOF mass spectrometer equipped with a high-performance solid-state laser (λ 355 nm) and a reflector. The system is operated by the Flexcontrol version 2.4 software packages (Bruker Daltonics GmbH, Bremen, Germany). Samples were irradiated with a laser power of 25–50 % and measured in the linear and the reflectron modes, in positive and negative ion modes. For tandem time-of-flight LIFT mode, 8.0 kV as ion source voltage was used with a precursor ion mass window of 3 Da.

The glycopeptides mixtures obtained after trypsin digestion were purified according to Selman et al. [45]. The enriched glycopeptides were resuspended in 50 % (v/v) acetonitrile in 1 % (v/v) formic acid. The samples were loaded onto an AnchorChip target (Bruker Daltonics GmbH) with α-cyano-4-hydroxycinnamic acid as matrix.

External calibration reagents used were (commercial proteins bradykinin 1–7, *M*r 757.399; angiotensin I, *M*r 1296.685; renin substrate, *M*r 1758.933; and insulin β chain, *M*r 3494.6506), β-cyclodextrin (cycloheptaamylose, *M*r 1135.0), and γ-cyclodextrin (cyclooctaamylose, *M*r 1297.1) with α-cyano-4-hydroxycinnamic acid as matrix in the positive ion mode.

Plant Material and Plant Inoculations

Orange (*Citrus sinensis* cv. Valencia late) was used as host plant for Xcc. All plants were grown in a growth chamber in incandescent light at 25 °C with a photoperiod of 14 h. Overnight cultures of Xcc strains were diluted in 10 mM

$MgCl_2$ to a final concentration of 10^5 CFU/ml. Plant inoculation and *in planta* growth assays were performed as previously described by Petrocelli et al. [41].

Statistical Analysis

Data were subjected to a bifactorial ANOVA test for adhesion and biofilm formation and to a unifactorial ANOVA test for EPS production. Tukey's multiple comparison tests with residual analysis and validation were also used in both cases. The analysis of growth curves *in planta* was performed using a mixed non-linear regression model with residual analysis and validation. Each experiment was repeated at least three times to ensure the reproducibility and consistency of the results.

Results

Construction of *pilA* Mutant from Xcc

Xcc genome sequence revealed the presence of three pilus-related genes: *pilA* (XAC3805) and *fimA/A1* (XAC3240-XAC3241) that encode pilin-like proteins. A detailed in silico analysis of these genes and of the secondary structure of pilin proteins was performed and described in Online Resource 2. In addition, phylogenetic analysis of genes that encode pilin proteins of *Xanthomonas, Xylella*, and *Stenotrophomonas* genus revealed a clear distinction between *pilA* and *fimA* genes, clustering on different clades (Online Resource 3).

A *pilA* mutant strain from *Xcc* (*XccΔpilA*) was generated by insertional inactivation of the gene due to the introduction of a streptomycin/spectinomycin resistance cassette through a double crossover. Growth of liquid cultures in SB medium was spectrophotometrically monitored by optical density at 600 nm (OD600). No differences in growth curves were observed between Xcc wt and *XccΔpilA* after a 48 h period (Online Resource 4).

XccΔpilA Exhibits Different Motility Patterns Compared to Xcc wt

In this work, we evaluated the effect of the *pilA* mutation on bacterial flagella-dependent motilities by performing swimming and swarming assays on 0.3 and 0.7 % (w/v) SB agar plates, respectively. As shown in Fig. 1a, swimming motility capability was reduced for *XccΔpilA* mutant compared to Xcc wt, recovering the migration ability in the complemented strain *XccΔpilA(pBBad22K)*. When swarming was analyzed, higher migration diameters were observed for Xcc wt compared to *XccΔpilA*, showing that the colony border appearance presented some differences

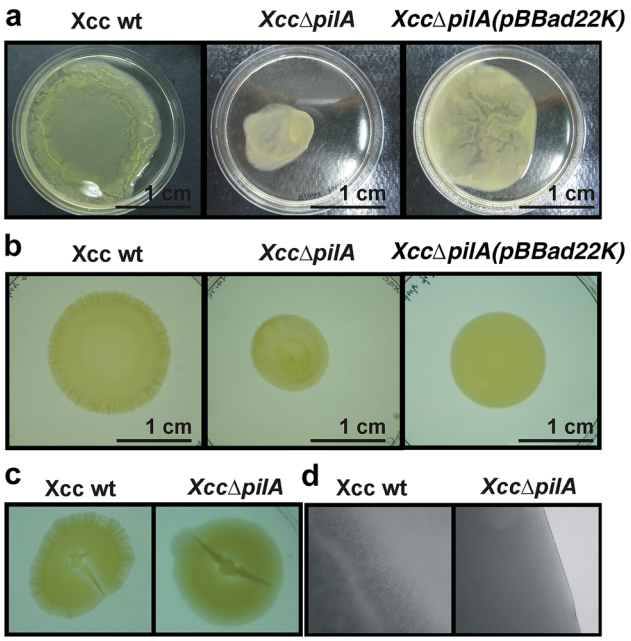

Fig. 1 Bacterial motility assays. The different strains were centrally inoculated on SB plates supplemented with 0.3 % (w/v) agar for swimming (**a**) and 0.7 % (w/v) agar for swarming (**b**) assay and incubated 72 h at 28 °C. For twitching motility assay, Xcc strains were stab-inoculated with a sterile toothpick through SB 1 % (w/v) agar plates to the bottom of the Petri dish. **c** Macroscopic and **d** microscopic analysis of colony borders morphology after incubation at 28 °C for 24 h. An optic Olympus BX40 microscope equipped with an Olympus camera system was used in **d**

(Fig. 1b). *XccΔpilA(pBBad22K)* partially recovered the migration capacity of the Xcc wt. We also observed that *XccΔpilA* colonies presented a significantly lower production of EPS ($P < 0.05$) than the wt and complemented strains (Table 1).

Although no differences in the migration capability were observed in 1 % (w/v) SB agar plates (which, in fact, are conditions commonly used for twitching motility evaluation), Xcc wt colony borders presented a particular pattern similar to the bacterial rafts described for some twitching-performing bacteria (Fig. 1c). The assessment of twitching motility by colony morphology is commonly used in plant pathogenic bacteria [2, 25]. On the other hand, *XccΔpilA*

Table 1 Exopolysaccharide production of Xcc strains in liquid medium

Bacterial strains	[EPS] (mg/ml)
Xcc wt	$3.8 \pm 0.6^{*}$
XccΔpilA	$2.7 \pm 0.5^{**}$
XccΔpilA(pBBad22K)	$3.9 \pm 0.5^{*}$

Data are expressed as means ± standard errors of three independent experiments

*,** Statistically significant differences ($P < 0.05$)

colony shapes were round and showed smooth borders without bacterial extensions radiating in these growth conditions (Fig. 1c). In addition, a bacterial disorganization on the edge of the twitching zones for Xcc wt was observed when a microscopic analysis was performed. In contrast, *pilA* mutant presented a smooth border and no displacement of bacteria from the main body of the colony (Fig. 1d).

Bacterial Adhesion and Biofilm Formation Decrease in the *XccΔpilA*

When the effect of *pilA* mutation on the attachment to abiotic and biotic surfaces was studied, the mutant strain presented a significantly reduced adhesion capacity to a plastic surface and to the abaxial face of orange leaves compared to Xcc wt and *XccΔpilA(pBBad22K)* ($P < 0.05$) (Fig. 2a, b).

In order to evaluate the aggregation of bacterial cells of Xcc wt, *XccΔpilA*, and *XccΔpilA(pBBad22K)*, biofilm formation was assayed on glass tubes containing SB liquid medium. After 3 and 6 days of static incubation at 28 °C, *XccΔpilA* showed significantly lower cell aggregates and adhesion on the air–liquid interface than Xcc wt. An intermediate behavior was observed for *XccΔpilA(pBBad22K)*. These results were corroborated by CV staining and quantification (Fig. 2c).

Deletion of *pilA* Gene from Xcc Modifies the Levels of Pilin Glycosylation

The in silico analysis of the genes related to the structural subunit of Tfp from Xcc indicated that *fimA/A1* and *pilA* genes present differences in their nucleotides composition, which is manifested in minor variations in the composition of their respective proteins in comparison to other bacteria from *Xanthomonas* genus. Although these differences are small, it allows separating the *X. citri* of *X. oryzae* and *X. campestris* clades with accuracy (Online resource 3).

To get some insight into the Xcc Tfp structure, partially purified Tfp fractions from the wt and the mutant strains were obtained. Interestingly, the SDS-PAGE profiles of these fractions showed that in both strains only one low migrating band was strongly stained with periodic acid–Schiff, indicating the glycoprotein nature of this component (Online Resource 5). In order to confirm this fact, the sugar components of the trypsin-released peptide mixture from Xcc wt and the mutant strains were hydrolyzed with 2 N TFA and subjected to HPAEC-PAD (Fig. 3a, b). Both samples presented glucose as the main component and mannose as the minor one but in different relationships. The peak with retention time 3.2 min may correspond to a substituted monosaccharide.

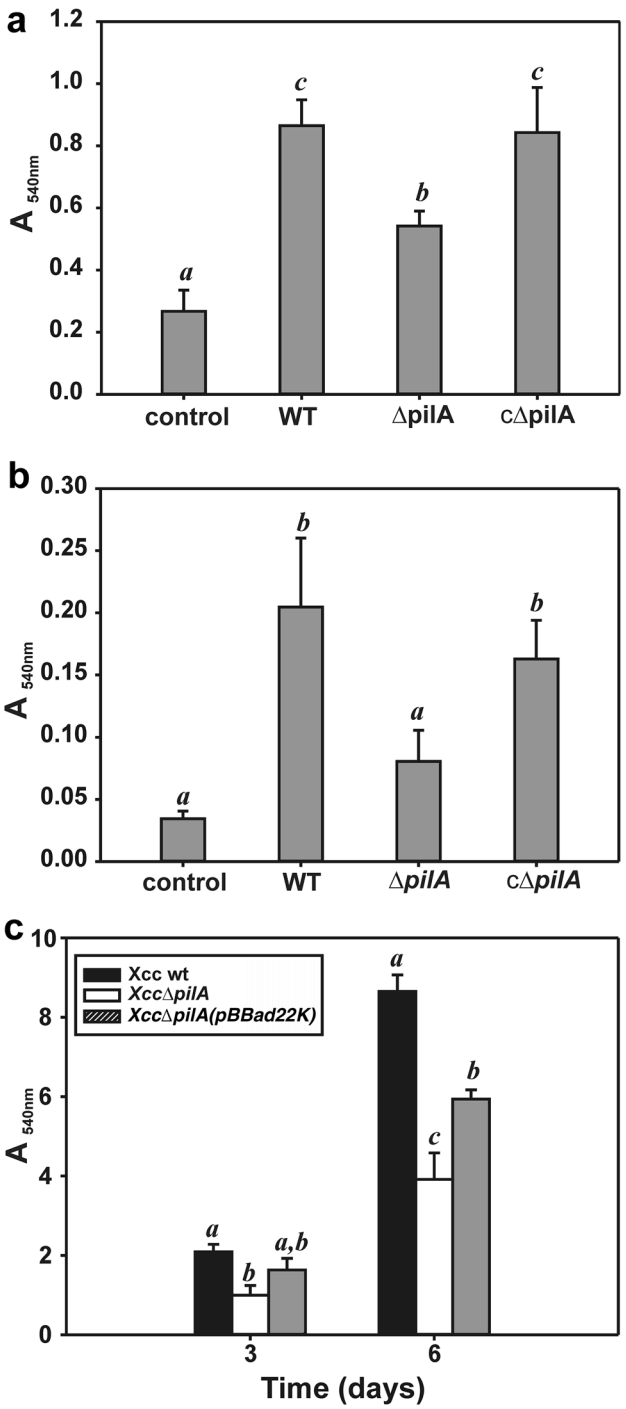

Although peptide hydrolysis was almost complete, a peak with a bigger retention time than the expected for a monosaccharide was detected. Therefore, it was collected and further analyzed by MALDI-TOF mass spectrometry in the positive reflectron mode (Fig. 3c). Signal at *m/z* 680.2 (calc. *m/z* 681.2448, $C_{25}H_{45}O_{21}$) corresponded to a tetrasaccharide bearing a methyl substituent as $[M + H]^+$. In accordance, ions at *m/z* 622.8 (calc. *m/z*621.8) and *m/z* 562.7 (calc. *m/z* 563.7) could be ascribed to $^{0,2}A_1$ and $^{2,5}X_1$

◀**Fig. 2** Bacterial adhesion to abiotic and biotic surfaces. **a** Bacterial adhesion on plastic (polystyrene microtiter plate) surface of Xcc wt (WT), *XccΔpilA* (ΔpilA) and *XccΔpilA(pBBad22K)* (cΔpilA) strains grown in XVM2 medium. **b** Bacterial adhesion on abaxial orange leaf surfaces. Histograms represent spectrophotometric quantifications of CV attached to the different surfaces (Abs 540 nm). Data are expressed as means ± standard errors of three independent experiments. Statistically significant differences are identified by *lowercase letters* ($P < 0.05$). **c** Biofilm formation on glass tubes. Xcc strains were statically grown on glass tubes at 28 °C. The adhered cells to the glass surface after 3 and 6 days of incubation were stained with CV. The resulting CV bound to these cells was quantified by measuring absorbance at 540 nm and represented on the histogram. Data are expressed as means ± standard errors of three independent experiments. Statistically significant differences are identified by *lowercase letters* ($P < 0.05$) at each time

fragments, respectively [13]. Furthermore, ion at *m/z* 505.6 (calc. *m/z* 505.1763, $C_{18}H_{33}O_{16}$) matched the same structure after the loss of a methylated hexose unit and signal at *m/z* 447.5 (calc. *m/z* 447.2) agrees with the corresponding $^{0,2}A_1$fragment. To obtain more details about the oligosaccharide structure of both Tfp, gel bands corresponding to Xcc wt and *XccΔpilA* were subjected to a reductive β-elimination. The released oligosaccharides were analyzed by HPAEC-PAD. As expected, peaks with retention times similar to reduced maltose, maltotriose, and maltotetraose were detected in both strains indicating that oligosaccharides composed of 2–4 hexose units were present in both samples (Fig. 3d).

A MALDI-TOF mass spectrometry analysis of the trypsin-digested fractions was further performed in the positive reflectron mode (Fig. 4). No differences were observed between the spectra of the total peptide fraction (not shown) and the glycopeptide fraction obtained after an enrichment step using HILIC-SPE chromatography, indicating that Xcc wt and *XccΔpilA* pilins are highly glycosylated. Taking into account the known sequences of FimA, FimA1, and PilA, we were able to ascribe signals to different glycopeptides in the spectra of both samples (Fig. 4a, b). The highest ion detected in both strains corresponded to *m/z* 832.80 (calc. *m/z* 832.38) and to peptide 116–120 (calc. *m/z* 646.3671) substituted with a hexose unit as $[M + Na]^+$. The fact that FimA1 and FimA share the same peptide (LTWAR or ITWAR) would account for the high intensity of this ion. Regarding FimA, signal at *m/*

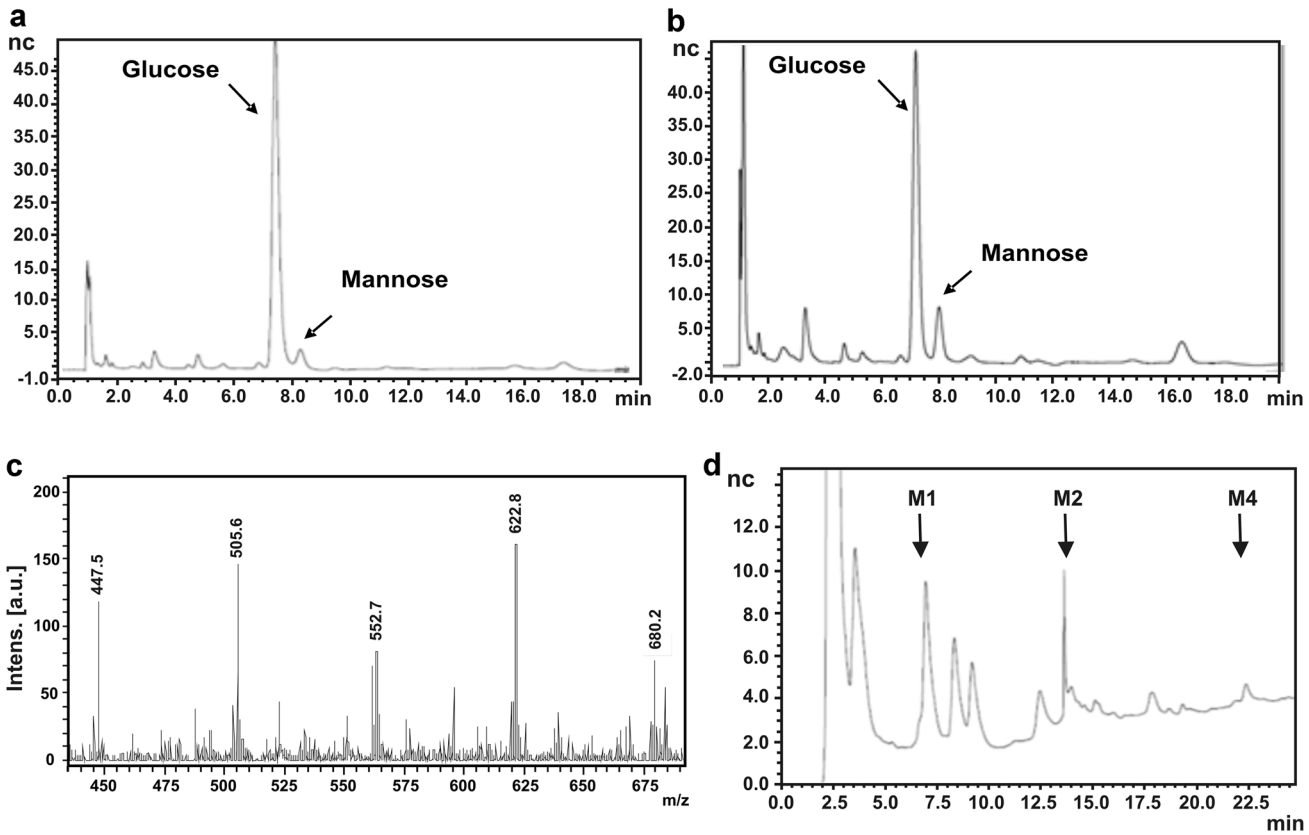

Fig. 3 HPAEC-PAD analysis of the monosaccharide composition of Tfp from Xcc strains. Mixtures of the sugar components of the trypsin-released peptides from Xcc wt (**a**) and *XccΔpilA* (**b**) were totally hydrolyzed with 2 N trifluoroacetic acid and subjected to HPAEC-PAD under optimal conditions for neutral and amino sugars. **c** MALDI-TOF mass spectrum of the component migrating as oligosaccharides from figures (**a**) and (**b**). **d** HPAEC-PAD analysis of the oligosaccharides released by reductive β-elimination from the gel band corresponding to Tfp from Xcc wt

z 1475.57 (calc. *m/z* 1475.76) corresponded to peptide 39–52 (calc. *m/z* 1313.7060, ^{39}SQVAAGLAEVSPGK^{52}) substituted with a hexose unit and ion at *m/z* 1651.87 (calc. *m/z* 1651081) corresponded to the same peptide bearing another monomethyl hexose unit; ion at *m/z* 2282.23 (calc. *m/z* 2282.07) matched peptide 121–139 (*m/z* 2119.0124, ^{121}DANGIWTCSTDLPLVDKDR^{139}) substituted with a hexose unit and signal at *m/z* 3153.41 (calc. *m/z* 3153.52) was ascribed to peptide 55-82 (*m/z* 2828.4160, ^{55}YEILVNDSEGSTLTSASAIGLTATATSR^{82}) bearing two hexose units.

On the other hand, other signals corresponding to FimA1 could be detected. Thus, ion at *m/z* 1519.48 (calc. *m/z* 1519.79) was ascribed to peptide 37–50 (*m/z* 1357.7322, ^{37}SQVTAGLAELSPGK^{50}) linked to a hexose unit; ion at *m/z* 1973.97 (calc. *m/z* 1973.85) matched peptide 121–137 (*m/z* 1797.7960, ^{121}DTNGVWTCSTDIATADK^{137}) bearing a monomethyl hexose; a signal at *m/z* 1996.97 corresponded to peptide 121–139 (*m/z* 1996.9280, ^{121}DTNGVWTC STDIATADKAK^{139}) and a signal at *m/z* 2164.30 (calc. *m/z* 2164.06) corresponded to the sodium adduct of peptide 62–81 (*m/z* 1979.0040, ^{62}GTTLTTADAVGLQATSTT

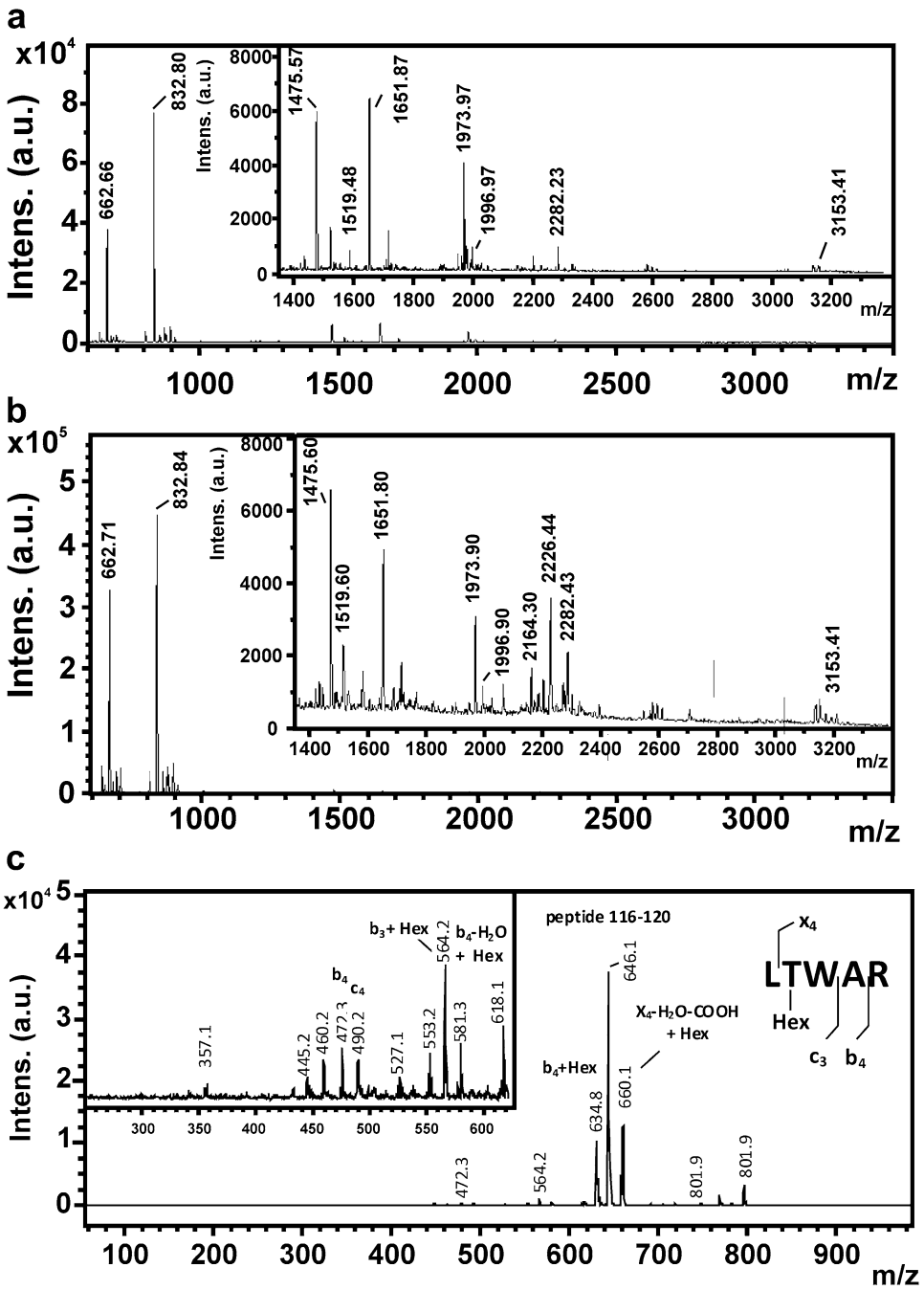

Fig. 4 MALDI-TOF mass spectra obtained after trypsin digestion. The glycopeptide fractions obtained from Xcc wt (**a**) and *XccΔpilA* (**b**) were trypsin-digested and enriched using HILIC-SPE chromatography before the MALDI-TOF mass spectrometry analysis was performed. *Insets* correspond to expanded range from *m/z* 1400 to 2100 Da. **c** The highest ion detected in the MALDI-TOF mass spectrometry analysis for both strains (*m/z* 832.80) was selected as precursor ion and subjected to laser-induced LID-MS/MS analysis. *Inset* corresponds to expanded range from *m/z* 100 to 620 Da

NR[81]) bearing a hexose unit. In order to ensure the presence of the glycosidic substitution, ion at *m/z* 832.80 was selected as precursor ion and subjected to laser-induced LID-MS/MS analysis in the MALDI-TOF/TOF MS/MS instrument (Fig. 4c). The spectrum showed a main ion at *m/z* 646.1 (calc. *m/z* 646.37) corresponding to the deglycosylated peptide 116–120. In addition, ions at *m/z* 634.8 and *m/z* 618.1 correspond to b_4 and b_4-H_2O fragments, respectively, bearing a hexose unit. In addition, ions at *m/z* 581.3 and 564.2 correspond to c_3 and b_3 fragments, respectively, linked to a hexose unit. Furthermore, *m/z* 490.2 corresponds to c_4 and *m/z* 472.3 to b_4 fragments.

XccΔpilA Develops Less Aggressive Disease Symptoms in Citrus Plants

In order to determine the effect of *pilA* mutation of Xcc on the development of citrus canker symptoms, orange leaves were infiltrated with 10^5 CFU/ml bacterial inoculums of Xcc wt, *XccΔpilA*, and *XccΔpilA(pBBad22K)* strains and the phenotypes developed were analyzed at different days post-inoculation (dpi). The lesion symptoms were smaller and less humid after 7 days for *XccΔpilA* when compared to Xcc wt. After 10 days, the mutant produced a reduced number of cankers in comparison to the wt strain and this difference was maintained after 15 days of infection (Fig. 5a). The differences in leaf damage may be associated with the bacterial growths inside the host tissue. The bacterial number of *XccΔpilA* recovered from the infected leaves at 20 dpi was significantly lower compared to Xcc wt and the complemented strain (Fig. 5b), indicating an association between *pilA* and the infection process.

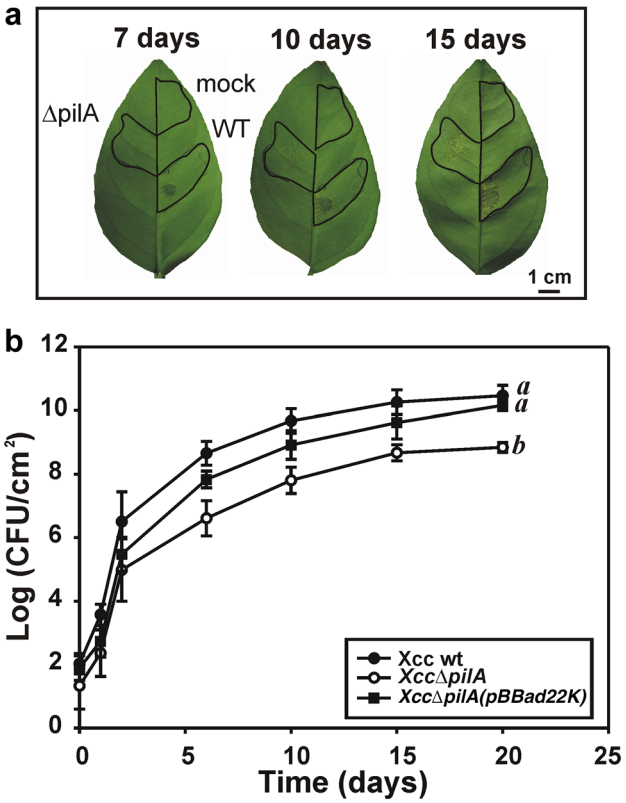

Fig. 5 Effect of *pilA* disruption on pathogenicity of Xcc in host plants **a** Progression of symptoms from the infiltration of 10^5 CFU/ml inoculums of Xcc wt, *XccΔpilA*, and *XccΔpilA(pBBad22K)* strains on abaxial faces of leaves is shown. The leaves were inoculated with 10 mM $MgCl_2$ as control (mock). Representative leaves after 7, 10, and 15 dpi are shown. *Scale bars*, 1 cm. **b** Growth curves on plant tissues were performed inoculating the leaves with 10^5 CFU/ml of Xcc strains. Data are expressed as means ± standard errors of three independent experiments. Statistically significant differences are identified by *lowercase letters* ($P < 0.05$)

Discussion

At present, few studies have assessed Type IV pili participation in pathogenesis processes and host colonization in bacterial plant pathogens [3]. Type IV pili functionality from *Xanthomonas citri* subsp. *citri* was recently evaluated [15]. The in silico analysis of Xcc genome revealed the presence of *pilA* and *fimA/A1* as structural components of the Tfp located in different *loci* in this bacterium. In addition, a great similarity was found between Tfp proteins from Xcc and from different species from the Xanthomonadaceae family, indicating that these proteins are important parts of the pili structure and/or biogenesis in this bacterium. A phylogenetic analysis of these genes revealed that *pilA* and *fimA/A1* belong to two distinct groups in all the bacteria analyzed. The differences in the phylogeny observed for each *Xanthomonas* species could be associated with the particular process of bacterial colonization that characterized each phytopathogen during the interaction with its host plant [6].

In this work, we have constructed a mutant strain in the *pilA* gene from *X. citri* subsp. *citri*, named *XccΔpilA*, in order to get insight into its role during citrus canker. Several reports showed that bacterial motility capability is affected in Tfp mutants in different phytopathogens [2, 39, 51]. In our work, we observed that *pilA* mutant from Xcc presented reduced migration during swimming and swarming motilities. It has been previously demonstrated that Xcc swarming motility depends on EPS secretion [22]. Accordingly, in this work, a minor production of exopolysaccharide was observed in *pilA* mutant, indicating that the lack of this gene affects these features in Xcc. A similar result was observed for a *Myxococcus xanthus pilA* mutant, resulting in a decrease of exopolysaccharide production [57].

It is well known that, in many animal and plant pathogenic bacteria, Tfp are essential for the flagella-independent twitching motility [2, 25, 26, 48]. The difference in the morphology of the colony borders and the bacterial organization between Xcc wt and *XccΔpilA* in the twitching zones indicates a reduced twitching capability for the mutant strain. Likewise, twitching-negative mutants with smooth colony borders were reported for *X. fastidiosa* [32]. Additionally, it was recently shown that *fimA1*, *pilB*, *pilZ*, *pilX*, and *fimX* mutants from *X. citri* subsp. *citri* had reduced subsurface twitching motility when compared to the wild-type strain [15]. Kuchma and colleagues postulated that other components of Type IV pili, named minor pilins, are required for swarming motility in *P. aeruginosa* [29]. These pilin-like proteins have conserved N-terminal sequences and are thought to be essential to pilus assembly and twitching motility in this bacterium [19]. In this context, PilA from *X. citri* subsp. *citri* could be incorporated into the Tfp and the variations on surface motilities observed for the *pilA* mutant could be explained by a role of this protein in the assembly of Tfp.

In addition to Tfp-dependent twitching motility, bacterial adhesion and biofilm formation have been described as important features for plant colonization [22, 36, 39]. In particular, the attachment to host tissue by cell surface adhesins and Type IV pili is an essential early event during the virulence process of several plant pathogens [36]. Tfp from *P. aeruginosa* and *P. syringae* pv. *tabaci* have been shown to induce bacterial adhesion and aggregation as well as twitching motility, achieving mature biofilms [19, 51]. Biofilm formation in Xcc appears as a complex and regulated process that depends on adhesion, EPS production, flagella-dependent motility and Tfp, as described in several reports [31, 33, 37, 58]. In this work, we observed a reduced adhesion capacity, differences in biofilm formation and reduced twitching capability for the mutant strain confirming that PilA from Xcc participates in the modulation of these features.

Besides, HPAEC-PAD together with MALDI-TOF MS analysis showed that Xcc Tfp are highly glycosylated. Glucose and mannose are the main components of the glycosidic portions of Tfp present in both strains. The presence of similar monosaccharide residues was detected in other bacterial pathogens [20]. It is known that protein glycosylation in bacterial pathogens influences interactions with their host. In *Neisseria* spp., Tfp glycosylation [1] was involved in host cell invasion [24]. Pilins of both *N. meningitides* and *N. gonorrhoeae* are glycosylated at a Ser amino acid by the attachment of a short oligosaccharide of up to three sugar residues in length [1]. Moreover, it was found that a glycan moiety, composed of a trisaccharide (N-hydroxybutyryl-N-formyl-Pse-xylose-N-acetylglucosamine), attached to the C-terminal Ser residue of PilA protein from *P. aeruginosa* 1244 was probably implicated in twitching motility and mouse colonization [8, 12, 49]. Protein glycosylation systems are also present in plant pathogens, such as *R. solanacearum.* It was demonstrated that Type IV pilins from this bacterium are glycosylated with the oligosaccharide HexNAc-(Pen)-dHex$_3$ that have the same structure of an O antigen subunit lipopolysaccharide. In *R. solanacearum*, the lack of glycosylation affected biofilm formation and virulence in tomato plant infections [17]. Further analysis performed in our work revealed the presence of a tetrasaccharide with a methyl substituent as the oligosaccharide present in Tfp from Xcc in contrast to the Tfp glycosidic portions found in the other bacteria analyzed. Despite these differences, the sugar substitution of pilin proteins from Xcc could be related to the physiology and the virulence of this bacterium.

Moreover, glycopeptides involving FimA and FimA1 sequences were detected. In the case of pilin subunits, this post-translational modification contributes to the structural complexity and functional diversification of Tfp [20]. In a recent report, Dunger et al. [15] suggested that *fimA1* is the main pilin gene of Tfp from Xcc expressed *in planta*, whereas *fimA* and *pilA* genes did not change their expression levels. Nevertheless, the results obtained from the glycosylation analysis provide the first experimental evidence that both FimA and FimA1 proteins are structural components of Tfp.

Type IV pili are involved in the early step of host tissue colonization during bacterial pathogenesis; however, the specific role is still unclear [5, 34]. Different results were described in relation to the participation of this structure in the host infectivity. Tfp from *Acidovorax avenae* ssp. *citrulli* and *P. syringae* pv. *tomato* DC3000 promote the colonization of their respective host plants [2, 5, 42, 51]. In *P. syringae* pv. *tabaci* 6605, Tfp were implicated not only in the host invasion but also in the hypersensitive reaction in non-host *Arabidopsis thaliana* leaves [51]. Mutants of *R. solanacearum* in Tfp-related genes, deficient in twitching motility, presented reduced autoaggregation and biofilm formation, lack of attachment ability to tobacco cells and to tomato roots and, they also produced less severe symptoms in tomato when compared to the wild-type strain [25]. Besides, *P. syringae* pv. *phaseolicola* wild-type and a *pilA* mutant strains inoculated into the host plant caused disease symptoms. However, only the wild-type strain produced halo blight disease in bean when the less invasive spraying method was used [43].

Although *Xanthomonas* genus includes several phytopathogen species, the contribution of Tfp to virulence has been studied only in few cases. Tfp mutants of the vascular pathogen *X. oryzae* pv. *oryzae*, unable to move by twitching, were deficient in biofilm formation and presented reduced virulence [10]. In addition to a reduced

virulence, mutants in the FimX and PilZ homologue of this bacterium presented a diminished hypersensitive response in non-host plants [56]. Furthermore, mutants defective in *pilA* gene, coding for the structural unit of Tfp from *X. campestris* pv. *campestris* showed an impaired surface motility and virulence [35].

A significant contribution of Tfp to virulence was shown for the non-vascular pathogen *X. oryzae* pv. *oryzicola* [54] and recently, a possible role of Tfp from Xcc in the pathogenesis process has been reported [15]. In our work, Xcc *pilA* mutant presented reduced plant colonization ability compared to the wild-type strain, which agrees with the results obtained for other Tfp mutants in different plant pathogens, supporting its role during citrus canker disease.

The contribution of PilA to surface motilities, adhesion, biofilm formation, and virulence indicates a functional role of this protein in Tfp from Xcc, corroborating the involvement of this structure in the infection process during citrus canker.

Acknowledgments We thank Catalina Anderson (INTA Concordia, Argentina), Gastón Alanis and Rubén Díaz Vélez (Proyecto El Alambrado) for the citrus plants, Sebastián Graziati for plant material support, the English Department (Facultad de Ciencias Bioquímicas y Farmacéuticas, UNR) for their assistance in the language revision of the manuscript and Biochemists Juan José Ivancovich and Hebe Bottai from Statistics and Data Processing Area (FBIOyF, UNR) for their assistance with statistical analysis. This work was supported by the Agencia Nacional de Promoción Científica y Tecnológica [ANPCyT PICT 2010-1762] to Elena G. Orellano and [ANPCyT PICT 2013-0736] to Alicia S. Couto.

References

1. Aas FE, Vik A, Vedde J, Koomey M, Egge-Jacobsen W (2007) *Neisseria gonorrhoeae* O-linked pilin glycosylation: functional analyses define both the biosynthetic pathway and glycan structure. Mol Microbiol 65:607–624
2. Bahar O, Goffer T, Burdman S (2009) Type IV Pili are required for virulence, twitching motility, and biofilm formation of *Acidovorax avenae* subsp. *citrulli*. Mol Plant Microbe Interact 22:909–920
3. Berry JL, Pelicic V (2015) Exceptionally widespread nanomachines composed of type IV pilins: the prokaryotic Swiss Army knives. FEMS Microbiol Rev 39:1–21
4. Brunings AM, Gabriel DW (2003) *Xanthomonas citri*: breaking de surface. Mol Plant Pathol 4:141–157
5. Burdman S, Bahar O, Parker JK, De La Fuente L (2011) Involvement of Type IV pili in pathogenicity of plant pathogenic bacteria. Genes 2:706–735
6. Buttner D, Bonas U (2010) Regulation and secretion of *Xanthomonas* virulence factors. FEMS Microbiol Rev 34:107–133
7. Casabuono A, Petrocelli S, Ottado J, Orellano EG, Couto AS (2011) Structural analysis and involvement in plant innate immunity of *Xanthomonas axonopodis* pv. citri lipopolysaccharide. J Biol Chem 286:25628–25643
8. Castric P, Cassels FJ, Carlson RW (2001) Structural characterization of the *Pseudomonas aeruginosa* 1244 pilin glycan. J Biol Chem 276:26479–26485
9. Da Silva AC, Ferro JA, Reinach FC, Farah CS, Furlan LR, Quaggio RB, Monteiro-Vitorello CB, Van Sluys MA, Almeida NF, Alves LM et al (2002) Comparison of the genomes of two *Xanthomonas* pathogens with differing host specificities. Nature 417:459–463
10. Das A, Rangaraj N, Sonti RV (2009) Multiple adhesin-like functions of *Xanthomonas oryzae* pv. *oryzae* are involved in promoting leaf attachment, entry, and virulence on rice. Mol Plant Microbe Interact 22:73–85
11. Daurelio LD, Romero MS, Petrocelli S, Merelo P, Cortadi AA, Talon M, Tadeo FR, Orellano EG (2013) Characterization of *Citrus sinensis* transcription factors closely associated with the non-host response to *Xanthomonas campestris* pv. *vesicatoria*. J Plant Physiol 170:934–942
12. DiGiandomenico A, Matewish MJ, Bisaillon A, Stehle JR, Lam JS, Castric P (2002) Glycosylation of *Pseudomonas aeruginosa* 1244 pilin: glycan substrate specificity. Mol Microbiol 46:519–530
13. Domon B, Costello CE (1988) A systematic nomenclature for carbohydrate fragmentations in FAB-MS/MS spectra of glycoconjugates. Glycoconj J 5:397–409
14. Dunger G, Arabolaza LN, Gottig N, Orellano EG, Ottado J (2005) Participation of *Xanthomonas axonopodis* pv. *citri hrp* cluster in citrus canker and in non-host plants responses. Plant Pathol 54:781–788
15. Dunger G, Guzzo CR, Andrade MO, Jones JB, Farah CS (2014) *Xanthomonas citri* subsp. *citri* type IV pilus is required for twitching motility, biofilm development, and adherence. Mol Plant Microbe Interact 27:1132–1147
16. Dunger G, Relling VM, Tondo ML, Barreras M, Ielpi L, Orellano EG, Ottado J (2007) Xanthan is not essential for pathogenicity in citrus canker but contributes to *Xanthomonas* epiphytic survival. Arch Microbiol 188:127–135
17. Elhenawy W, Scott NE, Tondo ML, Orellano EG, Foster LJ, Feldman MF (2016) Protein O-linked glycosylation in the plant pathogen *Ralstonia solanacearum*. Glycobiology 26:301–311
18. Friedman L, Kolter R (2004) Genes involved in matrix formation in *Pseudomonas aeruginosa* PA14 biofilms. Mol Microbiol 51:675–690
19. Giltner CL, Habash M, Burrows LL (2010) *Pseudomonas aeruginosa* minor pilins are incorporated into type IV pili. J Mol Biol 398:444–461
20. Giltner CL, Nguyen Y, Burrows LL (2012) Type IV pilin proteins: versatile molecular modules. Microbiol Mol Biol Rev 76:740–772
21. Gottig N, Garavaglia BS, Daurelio LD, Valentine A, Gehring C, Orellano EG, Ottado J (2008) *Xanthomonas axonopodis* pv. *citri* uses a plant natriuretic peptide-like protein to modify host homeostasis. Proc Natl Acad Sci USA 105:18631–18636
22. Gottig N, Garavaglia BS, Garofalo CG, Orellano EG, Ottado J (2009) A filamentous hemagglutinin-like protein of *Xanthomonas axonopodis* pv. *citri*, the phytopathogen responsible for citrus canker, is involved in bacterial virulence. PLoS One 4:e4358
23. Graham JH, Gottwald TR, Cubero J, Achor DS (2004) *Xanthomonas axonopodis* pv. *citri*: factors affecting successful eradication of citrus canker. Mol Plant Pathol 5:1–15
24. Jennings MP, Jen FE, Roddam LF, Apicella MA, Edwards JL (2011) *Neisseria gonorrhoeae* pilin glycan contributes to CR3 activation during challenge of primary cervical epithelial cells. Cell Microbiol 13:885–896
25. Kang Y, Liu H, Genin S, Schell MA, Denny TP (2002) *Ralstonia solanacearum* requires type 4 pili to adhere to multiple surfaces and for natural transformation and virulence. Mol Microbiol 46:427–437
26. Klausen M, Heydorn A, Ragas P, Lambertsen L, Aaes-Jorgensen A, Molin S, Tolker-Nielsen T (2003) Biofilm formation by

Pseudomonas aeruginosa wild type, flagella and type IV pili mutants. Mol Microbiol 48:1511–1524
27. Kraiselburd I, Alet AI, Tondo ML, Petrocelli S, Daurelio LD, Monzon J, Ruiz OA, Losi A, Orellano EG (2012) A LOV protein modulates the physiological attributes of *Xanthomonas axonopodis* pv. *citri* relevant for host plant colonization. PLoS One 7:e38226
28. Kraiselburd I, Daurelio LD, Tondo ML, Merelo P, Cortadi AA, Talon M, Tadeo FR, Orellano EG (2013) The LOV protein of *Xanthomonas citri* subsp. *citri* plays a significant role in the counteraction of plant immune responses during citrus canker. PLoS One 8:e80930
29. Kuchma SL, Griffin EF, O'Toole GA (2012) Minor pilins of the type IV pilus system participate in the negative regulation of swarming motility. J Bacteriol 194:5388–5403
30. Lee BM, Park YJ, Park DS, Kang HW, Kim JG, Song ES, Park IC, Yoon UH, Hahn JH, Koo BS et al (2005) The genome sequence of *Xanthomonas oryzae* pathovar *oryzae* KACC10331, the bacterial blight pathogen of rice. Nucleic Acids Res 33:577–586
31. Li J, Wang N (2011) Genome-wide mutagenesis of *Xanthomonas axonopodis* pv. *citri* reveals novel genetic determinants and regulation mechanisms of biofilm formation. PLoS One 6:e21804
32. Li Y, Hao G, Galvani CD, Meng Y, De La Fuente L, Hoch HC, Burr TJ (2007) Type I and type IV pili of *Xylella fastidiosa* affect twitching motility, biofilm formation and cell-cell aggregation. Microbiology 153:719–726
33. Malamud F, Homem RA, Conforte VP, Yaryura PM, Castagnaro AP, Marano MR, do Amaral AM, Vojnov AA (2013) Identification and characterization of biofilm formation-defective mutants of *Xanthomonas citri* subsp. *citri*. Microbiology 159:1911–1919
34. Mattick JS (2002) Type IV pili and twitching motility. Annu Rev Microbiol 56:289–314
35. McCarthy Y, Ryan RP, O'Donovan K, He YQ, Jiang BL, Feng JX, Tang JL, Dow JM (2008) The role of PilZ domain proteins in the virulence of *Xanthomonas campestris* pv. *campestris*. Mol Plant Pathol 9:819–824
36. Mhedbi-Hajri N, Darrasse A, Pigne S, Durand K, Fouteau S, Barbe V, Manceau C, Lemaire C, Jacques MA (2011) Sensing and adhesion are adaptive functions in the plant pathogenic xanthomonads. BMC Evol Biol 11:67
37. Moreira LM, Almeida NF Jr, Potnis N, Digiampietri LA, Adi SS, Bortolossi JC, Da Silva AC, da Silva AM, de Moraes FE, de Oliveira JC et al (2010) Novel insights into the genomic basis of citrus canker based on the genome sequences of two strains of *Xanthomonas fuscans* subsp. *aurantifolii*. BMC Genom 11:238
38. Murray MG, Thompson WF (1980) Rapid isolation of high molecular weight plant DNA. Nucleic Acids Res 8:4321–4325
39. Nguyen LC, Taguchi F, Tran QM, Naito K, Yamamoto M, Ohnishi-Kameyama M, Ono H, Yoshida M, Chiku K, Ishii T et al (2012) Type IV pilin is glycosylated in *Pseudomonas syringae* pv. *tabaci* 6605 and is required for surface motility and virulence. Mol Plant Pathol 13:764–774
40. Parente J, Casabuono A, Ferrari MC, Paggi RA, De Castro RE, Couto AS, Gimenez MI (2014) A rhomboid protease gene deletion affects a novel oligosaccharide N-linked to the S-layer glycoprotein of *Haloferax volcanii*. J Biol Chem 289:11304–11317
41. Petrocelli S, Tondo ML, Daurelio LD, Orellano EG (2012) Modifications of *Xanthomonas axonopodis* pv. *citri* lipopolysaccharide affect the basal response and the virulence process during citrus canker. PLoS One 7:e40051
42. Roine E, Raineri DM, Romantschuk M, Wilson M, Nunn DN (1998) Characterization of type IV pilus genes in *Pseudomonas syringae* pv. *tomato* DC3000. Mol Plant Microbe Interact 11:1048–1056
43. Romantschuk M, Bamford DH (1986) The causal agent of halo blight in bean, *Pseudomonas syringae* pv., attaches to stomata via its pili. Microb Pathog 1:139–148
44. Sambrook J, Fritsch EF, Maniatis T (1989) Molecular cloning: a laboratory manual. Cold Spring Harbor Laboratory Press, New York
45. Selman MHJ, Hemayatkar M, Deelder AM, Wuhrer M (2011) Cotton HILIC SPE microtips for microscale purification and enrichment of glycans and glycopeptides. Anal Chem 83:2492–2499
46. Semmler AB, Whitchurch CB, Mattick JS (1999) A re-examination of twitching motility in *Pseudomonas aeruginosa*. Microbiology 145:2863–2873
47. Simon R, Priefer U, Pühler A (1983) A broad host range mobilization system for in vivo genetic engineering: transposon mutagenesis in gram negative bacteria. Nat Biotechnol 1:784–791
48. Siri MI, Sanabria A, Boucher C, Pianzzola MJ (2014) New type IV pili-related genes involved in early stages of *Ralstonia solanacearum* potato infection. Mol Plant Microbe Interact 27:712–724
49. Smedley JG III, Jewell E, Roguskie J, Horzempa J, Syboldt A, Stolz DB, Castric P (2005) Influence of pilin glycosylation on *Pseudomonas aeruginosa* 1244 pilus function. Infect Immun 73:7922–7931
50. Sukchawalit R, Vattanaviboon P, Sallabhan R, Mongkolsuk S (1999) Construction and characterization of regulated L-arabinose-inducible broad host range expression vectors in *Xanthomonas*. FEMS Microbiol Lett 181:217–223
51. Taguchi F, Ichinose Y (2011) Role of type IV pili in virulence of *Pseudomonas syringae* pv. *tabaci* 6605: correlation of motility, multidrug resistance, and HR-inducing activity on a nonhost plant. Mol Plant Microbe Interact 24:1001–1011
52. Thieme F, Koebnik R, Bekel T, Berger C, Boch J, Buttner D, Caldana C, Gaigalat L, Goesmann A, Kay S et al (2005) Insights into genome plasticity and pathogenicity of the plant pathogenic bacterium *Xanthomonas campestris* pv. *vesicatoria* revealed by the complete genome sequence. J Bacteriol 187:7254–7266
53. Tondo ML, Petrocelli S, Ottado J, Orellano EG (2010) The monofunctional catalase KatE of *Xanthomonas axonopodis* pv. *citri* is required for full virulence in citrus plants. PLoS One 5:e10803
54. Wang L, Makino S, Subedee A, Bogdanove AJ (2007) Novel candidate virulence factors in rice pathogen *Xanthomonas oryzae* pv. *oryzicola* as revealed by mutational analysis. Appl Environ Microbiol 73:8023–8027
55. Wengelnik K, Bonas U (1996) HrpXv, an AraC-type regulator, activates expression of five of the six loci in the *hrp* cluster of *Xanthomonas campestris* pv. *vesicatoria*. J Bacteriol 178:3462–3469
56. Yang F, Tian F, Li X, Fan S, Chen H, Wu M, Yang CH, He C (2014) The degenerate EAL-GGDEF domain protein Filp functions as a cyclic di-GMP receptor and specifically interacts with the PilZ-domain protein PXO_02715 to regulate virulence in *Xanthomonas oryzae* pv. *oryzae*. Mol Plant Microbe Interact 27:578–589
57. Yang Z, Lux R, Hu W, Hu C, Shi W (2010) PilA localization affects extracellular polysaccharide production and fruiting body formation in *Myxococcus xanthus*. Mol Microbiol 76:1500–1513
58. Zimaro T, Thomas L, Marondedze C, Garavaglia BS, Gehring C, Ottado J, Gottig N (2013) Insights into *Xanthomonas axonopodis* pv. *citri* biofilm through proteomics. BMC Microbiol 13:186